The estimation of the values of ΔF_{D_i} can be made with the procedure described above. To make these estimations, it is necessary to have the detailed knowledge about the morphology of deposited particles; namely, the positions of each deposited particle. Such information can be obtained with the simulation model developed recently (Tien et al., 1977; Wang et al., 1977).

ACKNOWLEDGEMENT

This study was performed under Grant No. 79-05962, National Science Foundation.

NOTATION

a = Collector radius
b = Particle radius
C_D = Drag coefficient, Eq. 32
$C_{D,s}$ = Drag coefficient based on Stokes' law, Eq. 34
$f(\bar{r}_i, \bar{r}_j)$ = drag correction factor for the interaction between the i-th and j-th particles
$f(\bar{r}_1, \bar{r}_2 \ldots \bar{r}_N)$ = drag correction factor for the interaction among the N particles
$f_{\text{dendrite}}(n, \alpha)$ = drag correction factor for particle dendrite
F_D = Drag force
$F_{D,i}$ = Drag force on the i-th sphere
ΔF_D = Increase in drag force, Eq. 18
$\Delta F_{D,i}$ = Contribution to drag force increase due to the i-th particle
l = Center to center distance between two spheres
$N_{Re,o}$ = Reynolds number, $(2\, a\, U_o\, \rho/\mu)$
p = Pressure
p_{-n-1} = Spherical harmonic function of order $(n + 1)$
ΔP = Pressure drop
$\bar{r}$ = position vector in cylindrical polar coordinate
R_o = Radius of cylinder
R = radial coordinate
U = Approach velocity
U_o = Fluid velocity at cylinder axis
$U_{(o)}$ = z component of the undisturbed velocity field evaluated at the center of the particle, Eq. 9
$\bar{V}$ = Velocity field
W = Weight of the assembly subject to fluid flow
W_o = Weight of the assembly placed in fluid at rest
z = axial coordinate

LITERATURE CITED

Beizaie, M., "Deposition of Particles on a Single Collector," Ph.D Dissertation, Syracuse University, Syracuse, NY (1977).
Fayon, A. M., and J. Happel, "Effect of a Cylindrical Boundary on a Fixed Rigid Sphere in a Moving Viscous Fluid," *AIChE J.*, 6 (1960).
Ganatos, P., R. Pfeffer, and S. Weinbaum, "A numerical solution technique for Three-Dimensional Stokes' Flows with Application to the Motion of Strongly Interacting Spheres in a Plane," *J. Fluid Mech.*, **84**, 79 (1978).
Gluckman, M. J., R. Pfeffer, and S. Weinbaum, "A New Technique for Treating Multiparticle Slow Viscous Flow: Axisymmetric Flow Past Spheres and Spheroids," *J. Fluid Mech.*, **50**, 705 (1971).
Goldman, A. J., R. G. Cox, and H. Brenner, "The Slow Motion of Two Identical Arbitrarily Oriented Spheres Through a Viscous Fluid," *Chem. Eng. Sci.*, **21**, 1151 (1966).
Happel, J., and H. Brenner, "Low Reynolds Number Hydrodynamics," 2nd ed., Nordhoff, Leydeon (1973).
Lin, C. J., K. J. Lee, and N. S. Sather, "Slow Motion of Two Spheres in a Shear Flow," *J. Fluid Mech.*, **43**, 35 (1970).
Nir, A., and A. Acrivos, "On Creeping Motion of Two Arbitrary Sized Touching Spheres in a Linear Shear Field," *J. Fluid Mech.*, **43**, 35 (1970).
O'Neill, M. D., "On Asymmetric Slow Viscous Flows Caused by Motion of Two Equal Spheres Almost in Contact," *Proc.*, Camb. Phill. Soc., **65**, 543 (1969).
Payatakes, A. C., and C. Tien, "Particle Deposition in Fibrous Media with Dendrite-like Pattern: A Preliminary Model," *J. Aerosol Sci.*, **7**, 85 (1976).
Pendse, H., "A Study of Certain Problems in Deep Bed Filtration," Ph.D. Dissertation, Syracuse University, Syracuse, NY (1979).
Stimson, M., and G. B. Jeffery, "The Motion of Two Spheres in a Viscous Fluid," *Proc.*, Roy. Soc. (London), **A111**, 110 (1926).
Stokes, C. G., "On the Effect of the Internal Friction of Fluids on the Motion of Pendulums," *Trans.*, Cambr. Phill. Soc., **9**, pt. II, 8 (1851).
Tien, C., C. S. Wang, and D. T. Barot, "Chain-like Formation of Particle Deposits in Fluid Particle Separation," *Science*, **196**, 983 (1977).
Wang, C. S., M. Beizaie and C. Tien, "Deposition of Solid Particles on a Collector: Formulation of a New Theory," *AIChE J.*, **23**, 879 (1976).

Manuscript received February 26, 1980; revision received July 21, and accepted July 25, 1980.

Laminar Condensation Heat and Mass Transfer to a Moving Drop

This paper presents numerical solutions to the nonlinear, coupled boundary-layer equations governing laminar condensation heat and mass transfer in the vicinity of the forward stagnation point of a spherical cold water droplet translating in a saturated mixture of three components. The environment surrounding the droplet is composed of a condensable (steam), a noncondensable and nonabsorbable (air), and a third component which is noncondensable but absorbable (Elemental Iodine, for example). The dispersed and the continuous phases have been treated simultaneously. Results obtained here show excellent agreement with experimental results where available. An important conclusion is that for laminar condensation on a freely falling droplet, for a given thermal driving force and noncondensable gas concentration in the bulk, the dimensionless heat transfer decreases with increasing saturation temperature of the outside medium.

J. N. CHUNG

and

P. S. AYYASWAMY

University of Pennsylvania
Philadelphia, Pennsylvania 19104

SCOPE

In an earlier paper, Chung and Ayyaswamy (1978a) (hereinafter referred to as I) we have provided results for the forward stagnation point heat and mass transfer to a moving drop in the presence of laminar condensation. The theoretical development invoked two major simplifying assumptions. (a) The droplet inside could be treated as completly inviscid. Thus, the flow field inside the droplet was prescribed. The effect of

J. N. Chung is presently with the Department of Mechanical Engineering, Washington State University, Pullman, Washington 99163.

viscosity of the droplet liquid on the strength of the Hill's vortex inside the drop was not included. (b) The energy equation for the thermal boundary layer inside the drop did not include the contribution of the tangential component of convection. The motivation for invoking these assumptions was primarily to reduce the complexity in the mathematical structure of the problem.

Although these results are meaningful, the necessity for the development of a more refined theory which treats the dispersed phase in detail has never been ruled out. With the inclusion of the viscosity effects for the droplet-inside, three separate regions of flow can, in general, be discerned: an interior core flow; a boundary layer type flow near the surface of the drop; and an internal wake flow. The extent and strength of each type of motion depends on: (a) the ratios of the dynamic viscosities and of the densities of that of the droplet liquid and of the outside medium, and, (b) the Reynolds number characterizing the external flow (Batchelor, 1956; Harper and Moore, 1968; Chao, 1969; Harper, 1972).

For steady motion at high Reynolds number, the core is still a Hill's vortex (Batchelor, 1956), however, of a reduced strength. This strength is related to surface mobility. Prakash and Sirignano (1978) have found the strength of the liquid drop vortex in a vapor-gas stream to be about an order of magnitude smaller than that for a gas bubble. The thicknesses of the boundary layer and the internal wake have been shown to be of $0(Re^{-1/2})$ and $0(Re^{-1/4})$, respectively (Harper, 1972). Brignell (1975) has argued that the mass transfer inside the drop can also be viewed in a similar manner. In fact, it is easy to extend these arguments to heat transport also. We can, therefore, envision a thermal core in the interior, a thermal boundary layer near the surface, and an internal wake near the droplet central axis.

By a further extension of the analogy between mass and heat transfer inside the drop, the gradient in the thermal boundary layer can be shown to be much larger than that in the internal wake. It can also be analogously shown that the thermal boundary layer is a fast and efficient mechanism for the heat transfer, the internal wake is less efficient, and the drop interior core is less efficient still. The response times for the boundary layer, the internal wake and the interior core can be estimated to be in the ratio (R/U_s): $(R/U_s)\ Pe^{\frac{1}{2}}$: $(R/U_s)Pe$. Here, U_s is the maximum surface velocity and $Pe = (U_sR/\kappa_l)$, the drop Peclet number. For $Pe \sim 0(10^2)$ or more, we see that the boundary layer has the least response time.

In this paper, we offer results based on a refined theory that includes the effects due to the presence of hydrodynamic and thermal boundary layers inside the drop. The continuous phase theory is essentially the same as before with appropriate changes in the boundary and matching conditions. The changes in constraint conditions complicate the numerical study immensely as will be seen subsequently.

The droplet sizes and the thermodynamic range chosen for the illustrative calculations are closely related to the operating conditions that are likely to prevail in the containment spray atmosphere of a nuclear reactor following a loss-of-coolant accident. Apart from steam and air, the drop environment is taken to consist of Elemental Iodine (a typical fission product) in trace amounts. This investigation is, therefore, a contribution to the theory behind one aspect of nuclear safety—containment spray cooling system (Chung and Ayyaswamy, 1977; Tanaka, 1980).

CONCLUSIONS AND SIGNIFICANCE

Numerical solutions to the nonlinear, coupled boundary-layer equations governing laminar condensation heat and mass transfer in the vicinity of the forward stagnation point of a freely falling spherical cold water droplet in a saturated mixture of three components are presented. The environment surrounding the droplet is composed of a condensable (steam), a noncondensable and nonabsorbable (air), and a third component which is noncondensable but absorable (Elemental Iodine, for example).

The theoretical basis of this study is considerably more refined compared to I. The droplet-inside has been carefully treated and effects due to the presence of hydrodynamic and thermal boundary layers inside the drop are included in evaluating transport rates. Effect of viscosity on the internal core motion and the consequent reduction in the vortex strength inside the drop have been accounted for. The relationship between the continuous phase and the dispersed phase has been carefully defined. The interfacial shear stress continuity conditions have been identically satisfied by employing repeated iterative procedures.

With the inclusion of the viscosity effects for the droplet-inside, the convective velocity components are reduced by an order of magnitude compared to that of an Inviscid Hill's spherical vortex solution. The associated heat and mass transfer predictions are significantly smaller in magnitude (by as much as a factor of two in most cases). Excellent agreement of the present calculations with experimental results, where available, has been demonstrated, while the previous results had shown good comparison only in a qualitative sense. The most significant conclusion is that, for a translating droplet experiencing condensation, at a given thermal driving force and noncondensable gas concentration in the bulk, the dimensionless heat transfer decreases with increasing saturation temperature of the outside medium. Thermodynamic conditions suitable for the use of the well-established Ranz and Marshall correlation have been discussed in relation to results obtained here.

ANALYSIS

Consider a single, cold water spherical droplet initially of uniform temperature T_0, with fully developed and steady internal motion, that is translating at a constant velocity U_∞ in a large content of an otherwise quiescent mixture of its own vapor (steam, condensable), air (noncondensable and nonabsorbable), and a third component which is also a noncondensable but is absorbable. The third component is taken to be in trace amounts only. The mass transfer resistance for the transport of this third component is almost entirely in the gaseous phase. Let the mixture be at a temperature T_∞ ($T_\infty > T_0$), and the total pressure p_∞. The mass fractions of the noncondensable components in the bulk of the mixture are prescribed. The total pressure of the system is given by the sum of the partial pressures of the components in the bulk of the continuous phase. At the liquid and vapor-gas interface, the temperature T_i and mass fraction of each component are unknown *a priori* and are determined from two compatibility conditions that are explained in I.

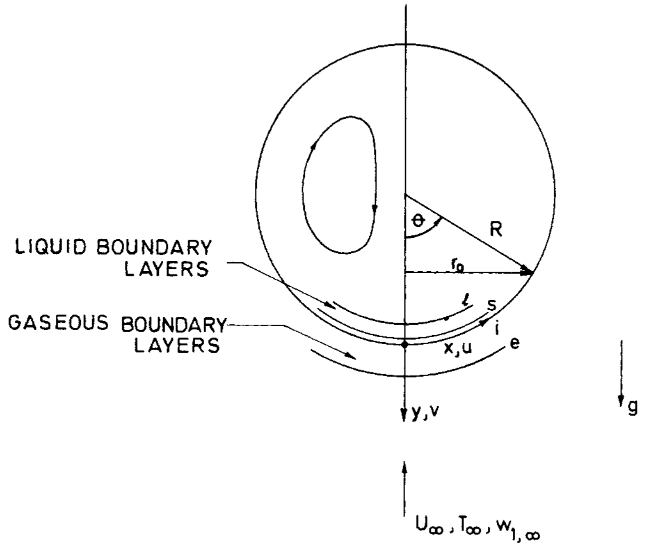

Figure 1. Geometry and coordinate system.

It is convenient to begin the analysis by separate considerations of each region in the model. We will also list the various assumptions where appropriate.

Region I: Liquid Region

(a) Inside the droplet, the flow field is taken to consist of a thin hydrodynamic boundary layer near the droplet surface, an internal wake near the central axis of the droplet and a Hill's vortex core flow with a reduced strength compared to that of a complete inviscid solution. This Hill's vortex is represented by:

$$\Psi_{\text{core}} = -\frac{1}{2} Ar^2(R^2 - r^2) \operatorname{Sin}^2\theta \tag{1}$$

Following Prakash and Sirignano (1978), $(U_\infty/AR^2) = 0(4 \sim 10)$, while this quantity is also a function of $(\mu_{\text{outside}}/\mu_{\text{inside}})$. In our problem, $(\mu_{\text{outside}}/\mu_{\text{inside}}) = 0(10^{-2})$. Therefore, from their theory $(U_\infty/AR^2) = 10$, the strength of the vortex is known. We have assumed that any reduction in the strength of the Hill's vortex is due only to the drop viscosity; i.e., the effect of condensation on the strength of the vortex is negligible. In fact, through an order of magnitude study, the inward momentum of the condensate can be shown to be at least an order of magnitude smaller than that of the surface motion. The thin hydrodynamic boundary layer will be assumed to be fully developed, steady and laminar (Chao (1969)).

(b) The thermal boundary layer within the droplet will be assumed to be fully developed and thin (Levich et al., 1965; Ruckenstein, 1967; Chao, 1969). Since the residence time along a closed stream line, which is also the residence time in the thermal boundary layer, is about two orders of magnitude smaller than the thermal diffusion time (Prakash and Sirignano, 1978), the thermal boundary layer can be treated as quasisteady.

(c) Since the flow velocity range to be considered is moderate, viscous dissipation, compressibility effects and expansion work can be neglected.

(d) No droplet oscillation.

The governing equations for the liquid boundary layers are, Figure 1:

$$\frac{\partial}{\partial x}(\rho_l u_l r_o) + \frac{\partial}{\partial y}(\rho_l v_l r_o) = 0, \tag{2}$$

$$\rho_l u_l \frac{\partial u_l}{\partial x} + \rho_l v_l \frac{\partial u_l}{\partial y} = \frac{\partial}{\partial y}\left(\mu_l \frac{\partial u_l}{\partial y}\right) + \rho_{l\infty} K_l^2\, x - L(\rho_l - \rho_{l\infty}) \tag{3}$$

$$\rho_l u_l \frac{\partial T_l}{\partial x} + \rho_l v_l \frac{\partial T_l}{\partial y} = \frac{1}{C_{pl}} \frac{\partial}{\partial y}\left(k_l \frac{\partial T_l}{\partial y}\right) \tag{4}$$

where

$$K_l = (U_\infty/10R),\ L = (gx/R)$$

The corresponding boundary conditions are:

$$u_l = (U_\infty/10R),\ T_l = T_{l,o} \text{ as } y \to -\infty$$

$$u_{l,i} = u_{vg,i},\ \mu \frac{\partial u_{vg,i}}{\partial y} = \mu_l \frac{\partial u_{l,i}}{\partial y},\ T_l = T_i \text{ at } y = 0 \tag{5}$$

We note that the appropriate boundary condition at the inside edge of the hydrodynamic boundary layer corresponds to the Hill's vortex, with strength $A = U_\infty/10R^2$, evaluated at the surface of the droplet $r = R$. The temperature at the edge of the thermal boundary layer is taken to be the instantaneous temperature of the outermost isothermal streamline of the internal thermal core.

The interfacial tangential velocity is governed by: (1) matching of shear stress and (2) continuity of tangential velocity. Thus, for the interfacial condensate layer, $u_{l,i} \to 0$ as $x \to 0$. Also, in view of the thinness of the condensate layer, the thermal resistance across it is sufficiently small that we can set $T_s \doteq T_i$.

Are we justified in assuming that the condensate layer is thin? Our analysis treats the entire problem as quasisteady. A dimensional analysis shows that this restricts the applicability to situations dealing with moderate rates of condensation. For moderate rates of condensation, by another dimensional reasoning, it is easy to demonstrate that the condensate layer in the vicinity of the forward stagnation point is thinner compared to the liquid boundary layer thickness. For example, we can estimate the time required to add one boundary layer thickness of condensate liquid on to the surface of the drop. For moderate rates of condensation, this time is much larger than the boundary layer response time and is, in fact, at least of the order of the core response time. Thus, for a quasisteady boundary layer analysis, the condensate liquid layer may to taken to be thin without introducing any appreciable error.

Alternatively, for a given ΔT, the thermal driving force $(\equiv T_\infty - T_o)$, we can develop an upper bound for the average thickness of the condensate layer. When the mechanism of heat transfer to the drop is taken to be entirely due to a change-of-phase (sensible heating excluded), we can estimate an upper bound for the mass transfer and then derive a corresponding thickness for the condensate layer. Such a bound yields $(\Delta R/R) \sim 1/3\, C_{pl}\, \Delta T/\lambda$. If $\Delta T = 50°\text{C}$, $C_{pl} = 1$ cal/g°C, $\lambda = 540$ cal/g, $(\Delta R/R) \sim 0.03$. If we took the sensible heat transfer into account, this estimate would be lower.

Also, even this thickness of the condensate layer can be deposited only over a long period (of the order of the core-response time). The assumption of a thin condensate layer is well justified. Since the continuous phase boundary layer is thicker than the liquid boundary layer, the condensate liquid layer is thinnest of the three. We should also note that in a condensing situation such as this, although there could be a large heat flux, the accompanying mass flux would be rather small. This is due to the large difference in densities between the liquid and the condensing vapor. We have taken the condensate liquid layer between s and i surfaces to be thin enough so that the thermal resistance across this condensate layer is sufficiently small. In effect, a conduction resistance across this thin layer has been suppressed.

Region II: Continuous phase boundary layer

The continuous phase boundary layer equations for ternary mixture are as given in I. The boundary conditions, however, have to be modified in the following manner:

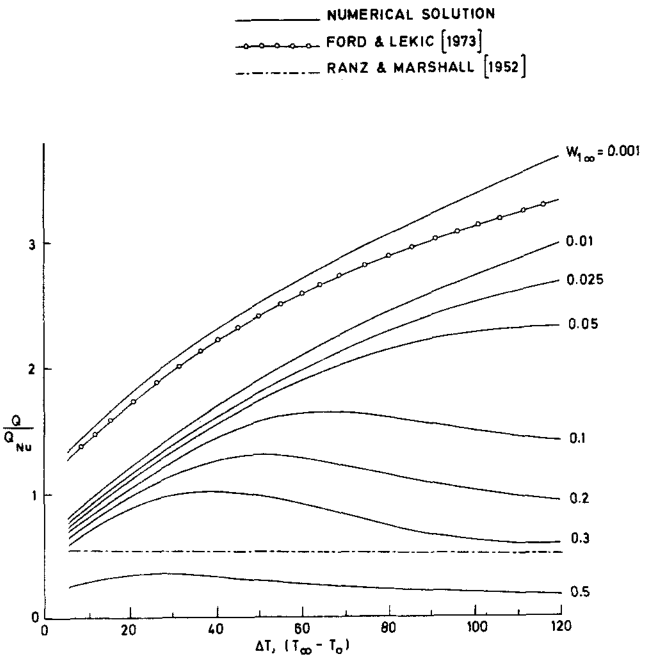

Figure 2. Effect of $w_{1,\infty}$ on condensation heat transfer: R = 0.025 cm, T_∞ = 125°C, 146 cm/s < U_∞ < 153 cm/s.

i-surface: $y = 0$

$$u_{vg,i} = u_{l,i} = GU_\infty \frac{x}{R},\ \mu \frac{\partial u_{vg,i}}{\partial y} = \mu_l \frac{\partial u_{l,i}}{\partial y},$$

$$v_{l,i} = 0,\ T = T_l = T_i \tag{6}$$

Here, G is a measure of the surface mobility. This is unknown and has to be determined through the use of the shear stress continuity condition. At the e-surface, the conditions are the same as in I. Compatibility conditions are also given in I.

SIMILARITY TRANSFORMATION

We introduce similarity variables appropriate to the liquid-side in addition to those given in I. The additional variables are:

$$\rho_l u_l = \frac{1}{r_o}\frac{\partial(\Psi_l r_o)}{\partial y},\ \rho_l v_l = -\frac{1}{r_o}\left(\frac{\partial \Psi_l r_o}{\partial x}\right),$$

$$\eta_l = yC_l^{1/2}/R,\ \Psi_l = \mu_{l\infty} C_l^{1/2}\, x\, f_l/R,\ \Theta_l = (T_l - T_i)/(T_\infty - T_i),$$

where

$$C_l = Re_{l\infty} = \frac{1}{10}\frac{U_\infty R}{\nu_{l\infty}}.$$

Consider writing,

$$f_l = f_{l0} + \epsilon f_{l1} + \ldots,\ \text{and},\ \Theta_l = \Theta_{l0} + \epsilon\Theta_{l1} + \ldots \tag{7}$$

The first-order equations for the liquid boundary layer are:

$$\left[\phi_{\mu l}\left(\frac{f'_{l1}}{\phi_{\rho l}}\right)'\right]' + 2f_{l0}\left(\frac{f'_{l1}}{\phi_{\rho l}}\right)' + 2f_{l1}\left(\frac{f'_{l0}}{\phi_{\rho l}}\right)' - 2\frac{f'_{l0}f'_{l1}}{\phi_{\rho l}} = 0(\epsilon^2), \tag{8}$$

and

$$\frac{1}{\phi_{c_{pl}} Pr_{l\infty}} (\phi_{kl}\Theta'_{l1})' + 2(f_{l0}\Theta'_{l1} + f_{l1}\Theta'_{l0}) = 0(\epsilon^2) \tag{9}$$

The corresponding boundary conditions are, i-surface:

$$f_{l1} = 0,\ 15\left(\frac{\mu}{\mu_l}\right)\left(\frac{C}{C_l}\right)^{1/2}\left(\frac{f'_1}{\phi_\rho}\right)' = \left(\frac{f'_{l1}}{\phi_{\rho l}}\right)',\ 15\left(\frac{f'_1}{\phi_\rho}\right) = \left(\frac{f'_{l1}}{\phi_{\rho l}}\right) = 10G_1,$$

$$\Theta_{l1} = 0,\ \eta = 0 \tag{10}$$

where $G = G_o + \epsilon G_l$, and, l-surface

$$\frac{f_{l1}}{\phi_{\rho l}} \to 0,\ \Theta_{l1} = 0,\ \eta_l \to -\infty. \tag{11}$$

The above sets of equations and boundary conditions are coupled with the continuous-phase equations and boundary conditions given in detail in I. Then, they are solved by the "quasilinearization" method. The entire set of equations have to be repeatedly iterated until the shear stress continuity conditions are identically satisfied and a unique G is determined for each set of parameter values. This complicated portion of the numerical procedure was not required in I in view of the neglect of the internal viscosity.

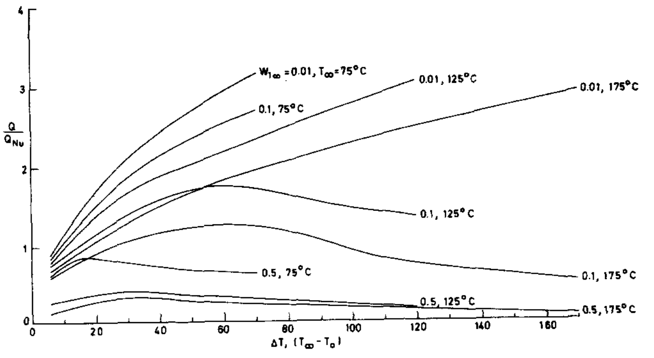

Figure 3. Effects of T and $w_{1,\infty}$ on condensation heat transfer: R = 0.025 cm; T_∞ = 175°C, 107 cm/s < U_∞ < 115 cm/s; T_∞ = 125°C, 146 cm/s < U_∞ < 153 cm/s; T_∞ = 75°C, 172 cm/s < U_∞ < 175 cm/s.

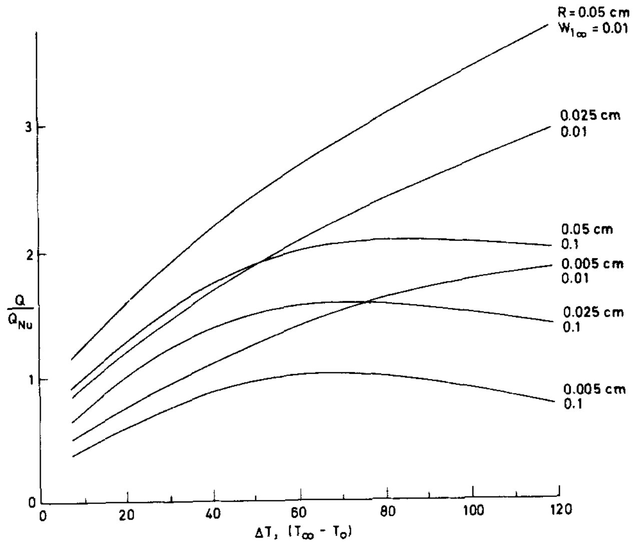

Figure 4. Effect of droplet radius R and $w_{1,\infty}$ on condensation heat transfer: T_∞ = 125°C; R = 0.05 cm, 322 cm/s < U_∞ < 335 cm/s; R = 0.025 cm, 146 cm/s < U_∞ < 153 cm/s; R = 0.005 cm, 23 cm/s < U_∞ < 25 cm/s.

RESULTS AND DISCUSSION

Heat transfer solutions for the translating drop problem are shown in Figures 2-4. The quantities Q_{Nu} and U_∞ have been explained in I.

In figure 2, the variation in the noncondensable gas mass fraction is in the wide range of $0.001 < w_{1,\infty} < 0.5$. The curves give (Q/Q_{Nu}) as a function of $(T_\infty - T_o)$ for various $w_{1,\infty}$. The radius R of the droplet is 0.025 cm. The free stream bulk

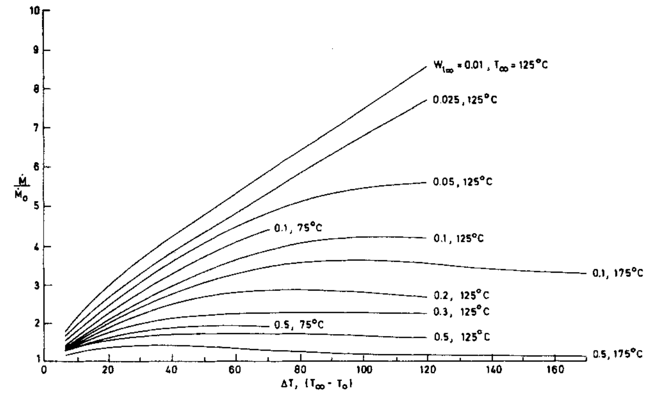

Figure 5. Effects of $w_{1,\infty}$ and T_∞ on the absorption of the third component, R = 0.025 cm.

temperature is taken to be 125°C. Comparison of Figure 2 here with Figure 2 of I shows that the heat transfer results of I were overpredicted by as much as a factor of two in several cases. With decreasing noncondensable gas in the bulk, the theory of I becomes increasingly inaccurate. The neglect of viscous effects in the dispersed phase has contributed to the high values reported in I.

A purely inviscid solution such as the one used for describing the velocity field inside the drop predicts convective velocity components which are about an order of magnitude higher than those realized in the present study and the transport results based on such a theory are likely to be exaggerated when dealing with liquid droplets in gas-mixture environments. With increasing mass fraction of the noncondensables in the bulk, the discrepancy between the present results and those of I are somewhat smaller. This is owing to the increasingly dominant presence of a new resistance in the continuous phase with increasing $w_{1,\infty}$.

Figure 2 shows the comparison between our results with the experimental results of Ford and Lekic (1973) and Ranz and Marshall (1952). Ford and Lekic's results are for condensation on drops in a pure steam atmosphere, and we would expect reasonable agreement with our results in the limit of $w_{1,\infty} \rightarrow 0$. In particular, the comparison with the case where $w_{1,\infty}$ forms a mere tenth of a percent of the mixture (0.1%) is seen to be excellent.

It should be realized that their results are for droplets approximately three times bigger than those investigated in the present study. Furthermore, they correspond to average heat transfer, while the present investigation provides stagnation point heat transfer. The stagnation point values will, of course, be higher. In I, we presented a similar comparison. However, the reported values for stagnation heat transfer in I were already about 40% higher than those predicted by experiments for a $w_{1,\infty}$ of 1%. With a much smaller $w_{1,\infty}$ such as a tenth of a percent, the comparison would have been worse. This is due to the noninclusion of the role played by viscosity.

But, an interesting question arises. How do we explain the close comparison of stagnation point results with an average result that is evident in Figure 2 of the present study? The effect of an inward condensation velocity is equivalent to that of suction, and this suction not only causes the boundary layers to be thin but also delays the onset of separation. The separation boundary layers are moved to the rear of the droplet, and the separation points are likely to be very close to the rear stagnation point. The effect due to separation on the condensation heat and mass transport would therefore be expected to be small.

Thus, theoretical and numerical predictions of transport based on the forward stagnation point for translating drops experiencing condensation may not differ significantly from average values for identical conditions. The chainline in Figure 2 corresponds to the Ranz and Marshall correlation that is used to describe the heat transfer from a droplet evaporating into a normal atmosphere. From the present investigation, it is seen that for the ambient thermal conditions and droplet size used in Figure 2, the correlations yields reasonable results only when about 30-50% of the drop environment consists of the noncondensable gas.

Figure 3 shows the variation of (Q/Q_{Nu}) with ΔT for different $w_{1,\infty}$ and for selected ambient saturation temperatures. The droplet size is 0.025 cm for given ΔT and $w_{1,\infty}$, the dimensionless heat transfer decreases with increasing ambient saturation temperature. This feature was first noted in I. The heat transfer values presented here differ considerably from those of I, particularly as $w_{1,\infty} \rightarrow 0$.

Figure 4 shows the variations of (Q/Q_{Nu}) with ΔT for various droplet sizes and $w_{1,\infty}$. The ambient thermal condition is fixed at 125°C. The droplet sizes vary from 0.005 to 0.05 cm. For a given ΔT and $w_{1,\infty}$, the dimensionless heat transfer increases with increasing radius. This is because with increasing droplet size, the flow field is more vigorous.

Figure 5 illustrates the effect of laminar film condensation on the transport of a noncondensable but absorbable third component in the mixture. In order to facilitate the mass transport discussion, we have introduced a reference mass flux $\dot{m}_0$. This reference flux is derived from a pseudophysical situation where a droplet is translating in a binary mixture of one component that has the same physical properties as steam but will not condense, while the other is a noncondensable but absorbable substance that exists in trace amounts (Chung and Ayyaswamy, 1978b).

For a given ΔT, the material transport of the third component decreases with increasing $w_{1,\infty}$. This is because, with increasing $w_{1,\infty}$, the build-up of the noncondensable in the close vicinity of the interface becomes significant enough to markedly slow down the condensation rate and the associated mass transport correspondingly decreases. For a given $w_{1,\infty}$, the mass transfer increases with increasing ΔT. This is attributable to the increased strength of the condensation flowfield which enhances the movement of the material towards the droplet interface. Again, the mass flux values of I are overpredictions when compared with the calculations based on a refined theory.

ACKNOWLEDGMENT

The authors would like to acknowledge the National Science Foundation for support under Grant ENG 77-23137.

NOTATION

A	= strength of the Hill's vortex as used in Eq. 1
C_p	= specific heat at constant pressure
D	= diameter of the droplet
f	= dimensionless stream function
g	= acceleration due to gravity
k	= thermal conductivity
$\dot{m}$	= mass flux
p	= pressure
Pr	= Prandtl number = ν/κ
Q	= heat flux
r_0	= radial distance from the axis of symmetry
r	= r-direction in spherical coordinate
R	= radius of droplet
Re	= Reynolds number = $(3/2)(U_\infty R/\nu_\infty)$ = C
T	= temperature
T_0	= droplet initial bulk temperature, instantaneous bulk temperature subsequently
u	= velocity in the x direction
v	= velocity in the y direction
U_∞	= terminal velocity of the droplet, free stream velocity
w	= mass fraction
x	= coordinate measuring distance along circumference from the stagnation point
y	= coordinate measuring radial distance outward from surface

Greek Letters

ΔT = $T_\infty - T_0$
ΔT_i = $T_\infty - T_i$
ϵ = mass fraction of third component in the bulk
η = similarity variable = $y\sqrt{c}/R$
θ = angle in spherical coordinates
Θ = dimensionless temperature
Θ_l = $(T_l - T_i)/(T_\infty - T_i)$
κ = thermal diffusivity = $k/\rho C_p$
λ = latent heat of vaporization
μ = dynamic viscosity
ν = kinematic viscosity = μ/ρ
ρ = density
ϕ_{C_p} = ratio $(C_p/C_{p\infty})$
ϕ_k = ratio (k/k_∞)
ϕ_μ = ratio (μ/μ_∞)
ϕ_ν = ratio $(2\nu_\infty/\nu_l)$
ϕ_ρ = ratio (ρ/ρ_∞)
Ψ = stream function

Subscripts

e = at outside edge of the continuous phase boundary layer
g = gas
i = at the dispersed-continuous phase interface
l = liquid
l, i = in the liquid at the interface
$,o$ = bulk condition in droplet
s = at the s-surface
v = vapor (steam)
v, i = in the vapor at the interface
vg, i = in the continuous phase at the interface
$_1$ = air
$_2$ = vapor or steam
$_3$ = noncondensable but absorable component
$_\infty$ = in the bulk phase, far away from the droplet

LITERATURE CITED

Batchelor, G. K., "On Steady Laminar Flow with Closed Stream Lines at Large Reynolds Number," *J. Fluid Mechanics*, **1**, 177 (1956).
Brignell, A. S., "Solute Extraction from an Internally Circulating Spherical Liquid Drop," *Int. J. Heat and Mass Transfer*, **18**, 61 (1975)..
Chao, B. T., "Transient Heat and Mass Transfer to a Translating Droplet," *J. Heat Transfer*, **91**, 273 (1969).
Chung, J. N., and P. S. Ayyaswamy, "The Effect of Internal Circulation on the Heat Transfer of a Nuclear Reactor Containment Spray Droplet," *J. Am. Nuc. Soc.*, **35**, No. 3, 603 (1977).
Chung, J. N., and P. S. Ayyaswamy, "Laminar Film Condensation Heat and Mass Transfer in the Vicinity of the Forward Stagnation Point of a Spherical Droplet Translating in a Ternary Mixture: Numerical and Asymptotic Solutions," *Int. J. Heat and Mass Transfer*, **21**, No. 10, 1309 (1978a).
Chung, J. N., and P. S. Ayyaswamy, "Material Transport with Steam Condensation on a Moving Spray Droplet Including the Effect of Internal Chemical Reaction," *Topics in Two-Phase Heat Transfer and Flow*, ed., Bankoff, S. G., 153, ASME, New York (1978b).
Ford, J. D., and A. Lekic, "Rate of Growth of Drops during Condensation," *Int. J. Heat and Mass Transfer*, **16**, 61 (1973).
Harper, J. F., and D. W. Moore, "The Motion of a Spherical Liquid Drop at High Reynolds number," *J. Fluid Mechanics*, **32**, 367 (1968).
Harper, J. F., "The Motion of Bubbles and Drops through Liquids," *Advances in Applied Mechanics*, **12**, 59 (1972).
Levich, V. G., V. S. Krylov, and V. P. Vorotolin, "On the theory of unsteady diffusion from moving drops," *Dokl. Akad. Nauk SSSR*, **161**, 648 (1965).
Prakash, S., and W. A. Sirignano, "Liquid Fuel Droplet Heating with Internal Circulation," *Int. J. Heat and Mass Transfer*, **21**, 885 (1978).
Ranz, W., and W. Marshall, "Evaporation from Drops," *Chem. Eng. Prog.*, **48**, 141, 173 (1952).
Ruckenstein, E., "Mass Transfer between a Single Drop and a Continuous Phase," *Int. J. Heat and Mass Transfer*, **10**, 1785 (1967).
Tanaka, M., "Heat Transfer of a Spray Droplet in a Nuclear Reactor Containment," *Nucl. Tech., J. Am. Nuc. Soc.*, **47**, No. 2, 268 (1980).

Manuscript received November 19, 1979; revision received July 21, and accepted July 25, 1980.

Local Hold-Up and Liquid Velocity in Air-Lift Reactors

Measurements of local hold-up and liquid recirculation rate in an air-lift reactor were performed with two types of gas spargers using a manometric technique. A simple exponential function correlated properly the liquid velocity measured to the gas flow rate. The local hold-up varied appreciably along the column and showed a maximum in most of the cases. A simple linear relationship correlated the local gas velocity with the total flow rate of the mixture.

JOSE C. MERCHUK
and
YEHUDA STEIN
Department of Chemical Engineering
Ben Gurion University of the Negev
Beer Sheva, Israel

SCOPE

Air-lift reactors have recently been the object of much attention, especially in relation to the production of single-cell proteins from hydrocarbons. The special feature that distinguishes an air-lift reactor from the more common one without mechanical agitation (bubble column) is the recirculation of the liquid through a downcomer that connects the gas-liquid separator on top of the main bubbling section or riser to its lower part. A net liquid flow develops in the riser and the downcomer. The main advantages of this design are the capacity for satisfying the very high oxygen demand of hydrocarbon fermentation (Wang, 1968), low energy input, especially in large configurations (Hatch, 1973; Legrys, 1977), and the possibility of easier removal of the heat generated in the fermentation process due to the configuration, especially in the case of external downcomers that act as heat exchangers (Schugerl et al., 1977).